Journal of Applied Polymer Science

Solution blowing of thermoplastic polyurethane nanofibers: A facile method to produce flexible porous materials

Yusuf Polat,[1] Esra Serife Pampal,[1] Elena Stojanovska,[1] Ramazan Simsek,[2] Ahmed Hassanin,[1,4] Ali Kilic,[1] Ali Demir,[1] Safak Yilmaz[3]

[1]Temag Labs, Department of Textile Engineering, Faculty of Textile Technology and Design, Istanbul Technical University, Istanbul, Turkey

[2]Department of Textile Engineering, Marmara University, Istanbul, Turkey

[3]Department of Mechanical Engineering, Istanbul Technical University, Istanbul, Turkey

[4]Department of Textile Engineering, Alexandria University, Alexandria, Egypt

Correspondence to: A. Kilic (E-mail: alikilic@itu.edu.tr)

ABSTRACT: Solution blowing (SB) is a promising and scalable approach for the production of nanofibers. Air pressure, solution flow-rate, and nozzle-collector distance were determined as effective process parameters, while solution concentration was also reported as a material parameter. Here we performed a parametric study on thermoplastic polyurethane/dimethyl formamide (TPU/DMF) solutions to examine the effect of such parameters on the resultant properties such as fiber diameter, diameter distribution, porosity, and air permeability of the nanofibrous webs. The obtained solution blown thermoplastic polyurethane (TPU) nanofibers had average diameter down to 170 ± 112 nm, which is similar to that observed in electrospinning. However, the production rate per nozzle can be 20 times larger, which is primarily dependent on air pressure and solution flow rate (20 mL/h). Moreover, it was even possible to produce nanofibers polymer concentrations of 20%; however, this increased the average nanofiber diameter. The fibers produced from the TPU/DMF solutions at concentrations of 20% and 10% had average diameters of 671 ± 136 nm and 170 ± 112 nm, respectively. SB can potentially be used for the industrial-scale production of products such as nanofibrous filters, protective textiles, scaffolds, wound dressings, and battery components. © 2015 Wiley Periodicals, Inc. J. Appl. Polym. Sci. **2016**, *133*, 43025.

KEYWORDS: electrospinning; fibers; membranes; polyurethanes; textiles

Received 4 August 2015; accepted 8 October 2015

DOI: 10.1002/app.43025

INTRODUCTION

Nanofibers have been widely investigated as materials for use in filtration, energy, textile, and biomedical applications. To date, methods such as electrospinning, meltblowing, phase separation, template synthesis, self-assembly, and spunbonding (island in the sea) have been proposed for the production of nanofibers. In particular, electrospinning has been widely utilized over the past two decades because of its simple operation.[1] To optimize the properties of nanofiber webs, various process parameters have been investigated, such as the applied voltage, solution flow-rate, distance between electrodes, and type of collector.[2] However, electrospinning has major limitations, such as safety problems (applied voltage of up to 60 kV) and low production rates (~1 mL/h/nozzle). Moreover, there are other drawbacks that are generally associated with the rheological and electrical properties of polymer solutions.[3]

Meltblowing is an established technology that is used to produce nonwoven materials from thermoplastic polymers. However, the die design is highly critical and the polymer flow-rate should be minimized to produce nanofibers.[4] Moreover, Ellison *et al.* observed the formation of particles, due to the frequent occurrence of fiber breakup, when maximized air to polymer mass flux ratios were used. This phenomenon was speculated to be driven by surface tension, which determines the fundamental limit for the meltblowing process.[5] Following their dissolution in proper solvents, polymers could be processed to reduce the effect of viscosity and surface tension, which would consequently reduce the average fiber diameter towards the nanoscale.[6–9] Coflowing compressed air jets, rather than electrostatic forces, stretch the dissolved polymer mass towards the collector to form polymeric nanofibers. Compared with electrospinning, the polymer throughput can be several times greater during solution blowing (SB), with much fewer restrictions due to the electrical properties of the solution. The solution blown fibers can be easily converted into a web that can be wound directly on a biological tissue or rotating cylinder, without the risk of electrical shock.[10]

Table I. Parameters for the Solution Blowing Process

Solution parameters	Viscosity[a] Polymer concentration[a] Molecular weight Surface tension Vapour pressure
Process parameters	Air pressure[a] Nozzle collector distance[a] Solution flow-rate[a]
System parameters	Nozzle diameter Nozzle geometry
Ambient	Temperature Humidity Atmospheric pressure

[a] Parameters studied in this work.

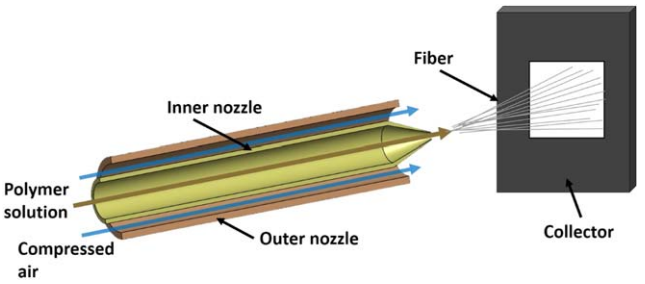

Figure 1. Schematic drawing of solution blowing (SB) apparatus used in this study. [Color figure can be viewed in the online issue, which is available at wileyonlinelibrary.com.]

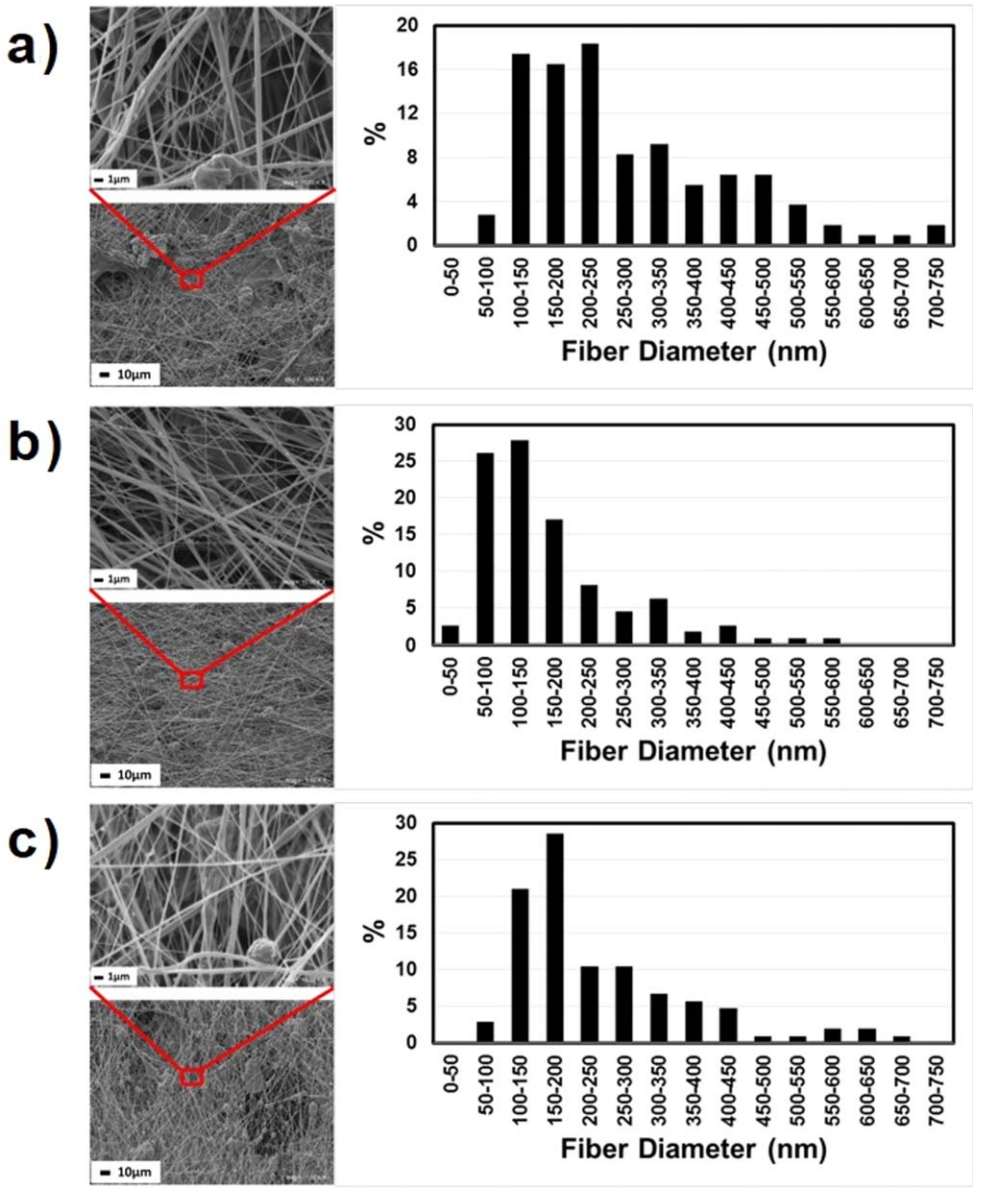

Figure 2. SEM images of solution blown TPU fibers produced at different air pressure values produced (a) 1 bar, (b) 3 bar, (c) 6 bar. [Color figure can be viewed in the online issue, which is available at wileyonlinelibrary.com.]

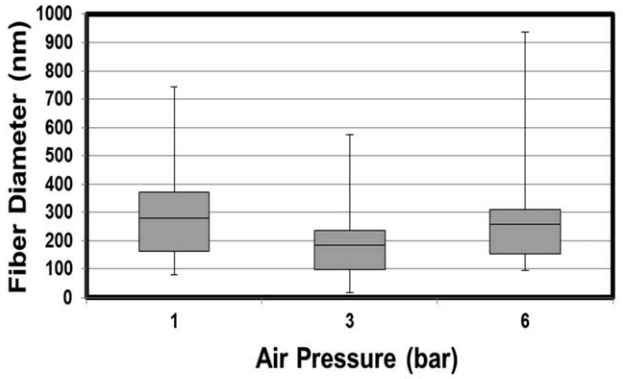

Parameters	Air pressure (bar)	Mean Diameter (nm)
Q= 10mL/h	1	279±115
d= 30cm	3	170±112
C= 10wt%	6	257±166

Figure 3. The box plot shows the relationship between air pressure and fiber diameter. The boundaries of the box indicate the 25th and 75th percentiles and the line indicates the median. The error bars above and below the box indicate the 95th and 5th percentiles. These data suggest that an air pressure of 3 bar is optimal to achieve a smaller fiber diameter with uniform distribution.

Several parameters, such as the solvent type, air pressure, viscosity, concentration, and distance between the collector and nozzle have important functions during the solution blow-spinning process. Considering this, Zhang *et al.*[6] investigated the effect of various solvents and solvent mixtures on the morphology of solution-blown polyvinyl pyrrolidone (PVP) fibers. Moreover, the relationship between the solvent and solution-blowing process parameters was also evaluated. Zhang *et al.*[6] reported that low air pressure does not allow solvent evaporation, which results in the accumulation of droplets on the collector. Conversely, high air pressure increases the turbulence of the airflow, and this randomly scatters the fibers, reducing the amount of fibers deposited on the collector. Thinner fibers are most affected by the turbulent air. In addition, a greater solution throughput increases the production rate; however, it increases the nanofiber diameter. Another drawback of high solution throughput is that droplets frequently form on the web, since the pressurized air cannot completely remove the solvent.[6] To decrease the level of droplet formation, Zhuang *et al.* used a heating unit that increased the evaporation rate of the solvent. Polymer flow rate increased abruptly, reaching to 18–48 mL/h where solution concentration ratio was in 5–20% range.[8]

To enhance the productivity further, Shi *et al.* utilized a die assembly, consisting of 20 orifices with a center-to-center distance of 5 mm, to produce polyvinylidene fluoride (PVDF) nanofibers. Two slits existed within the apparatus, where compressed air was blown over the polymer jet. When the solution reached the tip of the holes, the air jet forced it towards the collector. The resultant fibers exhibited a wavy orientation with an average diameter of 60–280 nm. Under an air pressure of 2.2 bar and a die-to-collector distance of 60 cm, the solution flow-rate per orifice was as high as 16 mL/h.[7]

Another study was conducted by Zhuang *et al.*,[9] in which solution-blown polyacrylonitrile (PAN) nanofibers were used as a precursor to produce carbon nanofibers. The average diameter of the obtained fibers was ~230 nm, which decreased to 136 nm following stabilization and carbonization procedures, because of the various gases that evolved. Carbon nanofibers are important engineering materials for Li-ion battery anodes, electromagnetic shielding, and composite applications.[9] The high throughput rate of SB may allow the rapid industrialization of carbon nanofibers.

In this study, a comprehensive optimization of parameters affecting SB process was performed for thermoplastic polyurethane (TPU). The limitations associated with SB, such as the reduction of the fiber diameter, minimization of droplet formation, and difficulties in collecting the nanofibers on the collector were investigated. Considering this, the process and material parameters listed in Table I were systematically varied. The morphology, permeability, and porosity of the solution-blown nanofibrous mats were also analyzed following each step.

EXPERIMENTAL

Materials

Polyester-based TPU C95 was purchased from BASF Corporation, Germany. As a linear segmented block polymer composed of hard and soft segments, TPU offers a versatile chemical structure, which enables it to be adapted for several applications such as textiles, membranes, protective clothing and filtration.[11–13] To determine the molecular weight of TPU, GPC analyses were carried out. The number average molecular weight was measured as 107,010 g/mol, with a polydispersity index (PDI) value of 1.81. Without any further treatment, *N,N*-dimethylformamide (DMF 98%) was used as a solvent to prepare the polymer solution. Neat polyurethane solutions (10, 15, and 20 wt %) were prepared by dissolving TPU pellets in DMF at 80°C.

Methods

A custom-made solution blowing (SB) apparatus was designed to realize the system shown in Figure 1. The air pressure was maintained between 1–6 bar, while the solution flow-rate was varied from 1–50 mL/h. The polymer solution was pumped through a 21-gauge needle, which was located inside a concentric nozzle ($d_i = 2$ mm) at a working distance of 15–50 cm. The polymer concentration was in the range of 10–20 wt %.

Characterization

Fiber Diameter. The morphology of the solution-blown nanofibers was examined using a Zeiss EVO MA10 scanning electron microscope (SEM) at 15.00–20.00 kV, with magnifications ranging from 500 to 20 k×. A tungsten filament was used to create the beam and the reported resolution was 35 Å under a 20 kV beam. Subsequently, 100 measurements were taken from 15 micrographs, and the average values and standard deviations were subsequently calculated. The IBM SPSS Statistics 22.0 program was used to verify the statistical significance of the parameters; the fiber diameter was determined to be dependent and the air pressure, solution flow-rate, distance, and concentration were determined to be independent. The most important

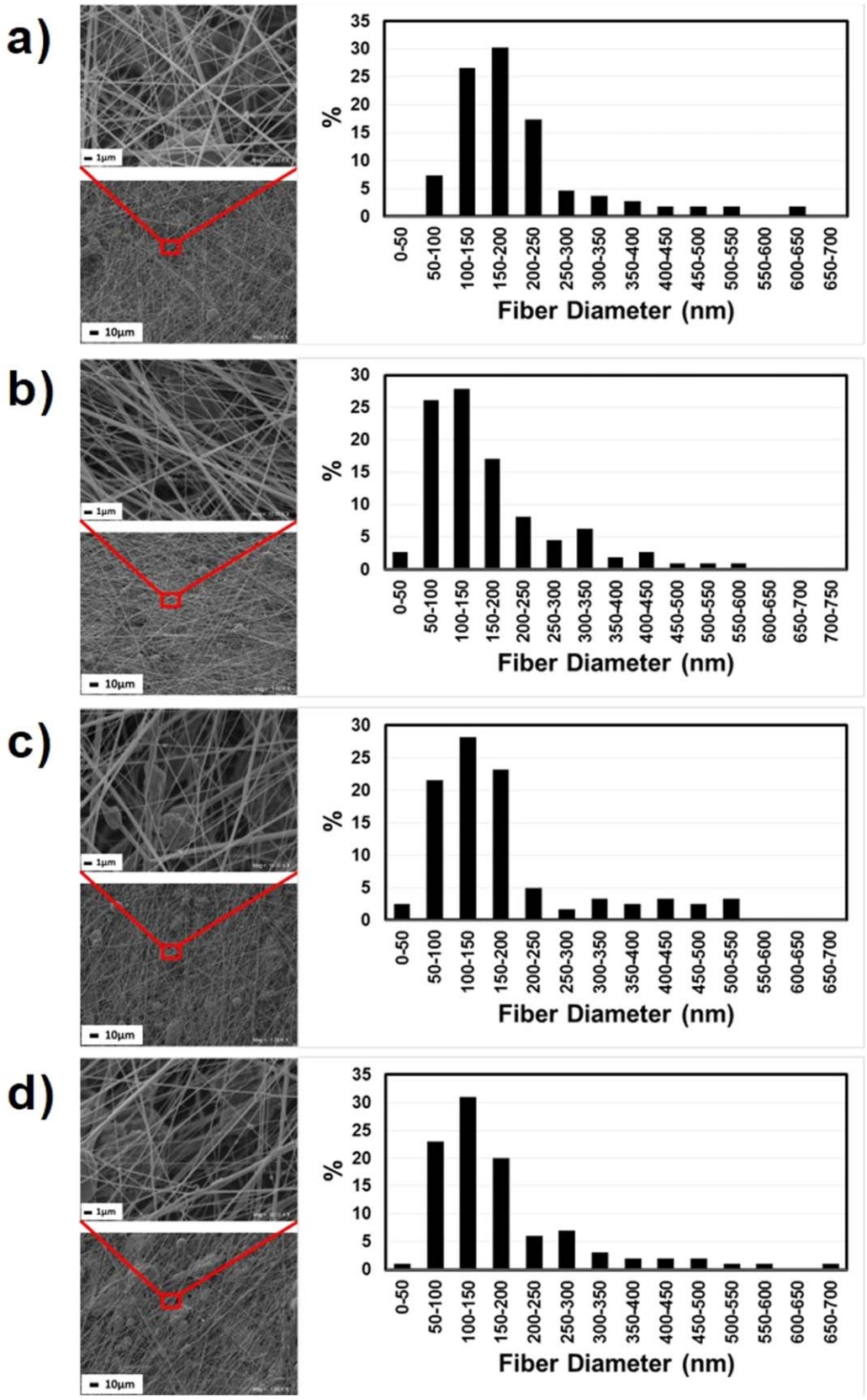

Figure 4. SEM images of solution blown TPU fibers with different flow-rate values produced (a) 1 mL/h, (b) 10 mL/h, (c) 25 mL/h, and (d) 50 mL/h. [Color figure can be viewed in the online issue, which is available at wileyonlinelibrary.com.]

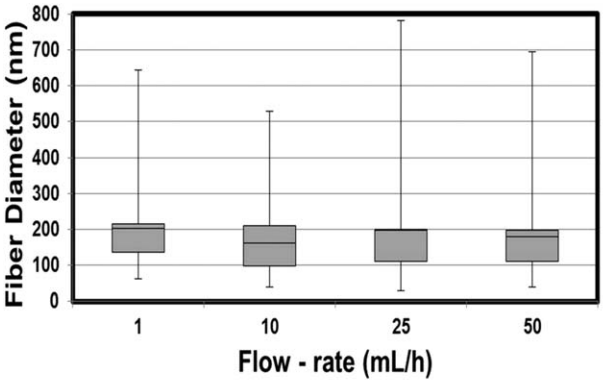

Parameters	Flow-rate (mL/h)	Mean diameter (nm)
P = 3bar d= 30cm C= 10wt%	1	203±111
	10	170±112
	25	198±158
	50	178±115

Figure 5. Fiber diameter vs. polymer solution flow-rate. The boundaries of the box indicate the 25th and 75th percentiles and the line indicates the median. The error bars above and below the box indicate the 95th and 5th percentiles. These data suggest that a flow rate of 10 mL/h is optimal to achieve smaller fiber diameters.

parameter was identified using the results of the Pearson correlation.

Air Permeability. The air permeability tests were conducted using the Prowhite Air Tester II. The tests were conducted according to ASTM D737 standards; following sealing, a sample with a surface area of 38 cm^2 was subjected to a pressure of 125 Pa.

Porosity. The Quantachrome 3Gwin capillary flow porometer was used to measure the pore size and pore size distribution. The nanofibrous webs were cut into circular shapes with a diameter of 1.8 cm. Porofil® with a defined surface tension of 16 mN/m was used as the wetting agent. The bubble point, mean flow pore size, mean pore size, and pore size distribution was calculated and obtained by the PSMWin Software. The pore size was calculated using the Young-Laplace formula:

$$P = \frac{4 \times \gamma \times \cos\theta}{D}$$

where P is the differential pressure, γ is the surface tension of the wetting liquid, θ is the contact angle of the wetting liquid, and D is the pore diameter.[14]

Viscosity. The share viscosity was measured with a Fungilab rotational viscometer at 25 ± 2°C temperature. Spindles R3, R5, and R6 were used for the polymer concentrations of 10, 15, and 20 wt %, respectively.

RESULTS AND DISCUSSION

In this report, the major parameters that affect the fiber morphology were systematically investigated and the fiber morphology and fiber diameter distribution were analyzed following each change. Finally, webs with fibers of various diameters were tested for potential use in barrier and filtration applications.

Effects of Air Pressure

The solution flow rate, nozzle-to-collector distance, and concentration were maintained at 10 mL/h, 30 cm, and 10%, respectively. The air pressure was altered to determine its effect on the fiber diameter and morphology. As shown in Figures 2 and 3, the air pressure did not have a linear influence on the nanofiber diameter. This could be because the low air pressure was not sufficient to evaporate the solvent, while the air turbulence generated at high pressure damaged the thin fibers, as reported in other studies.[6] Polymer agglomeration occurred at low air pressure, and solvent droplets could be observed throughout the entire sample because there was insufficient pressure to elongate the jet and evaporate the solvent during the flight of the fiber between the nozzle and collector. It was determined that an air pressure of 3 bar resulted in a lower concentration of droplets, and the smallest average diameter among all three samples; thus the air pressure was set to 3 bar to identify the optimal values for the other parameters. Moreover, the fiber diameter distribution narrowed at an air pressure of ~3 bar.

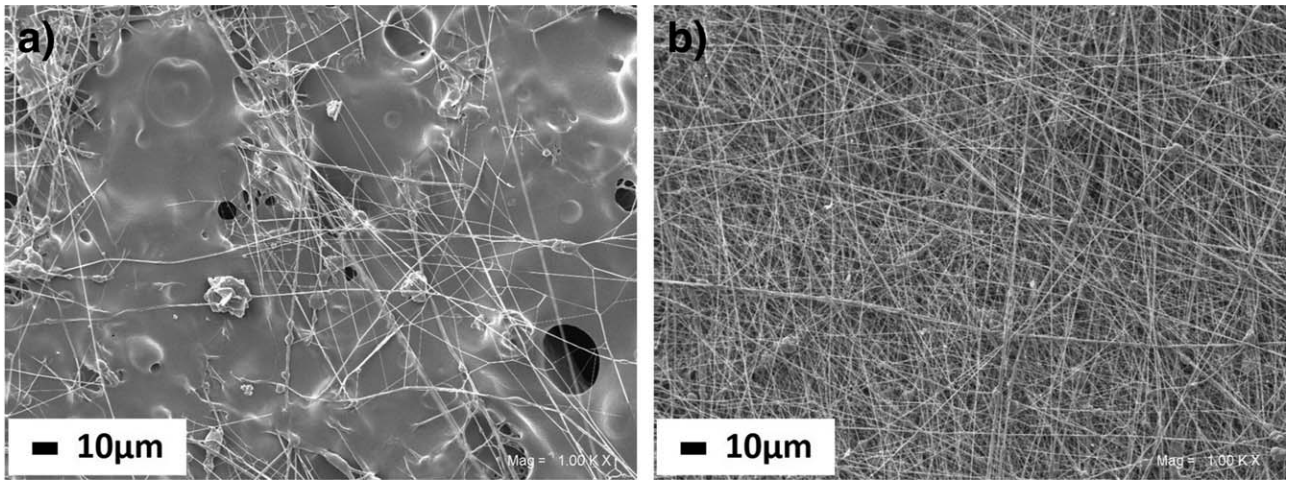

Figure 6. SEM images (×1000) of samples produced at a working distances of 15 cm (a) Image of central area of sample where the jet hits the collector (b) Image of an area located 3 cm from the central area where the jet strikes the collector.

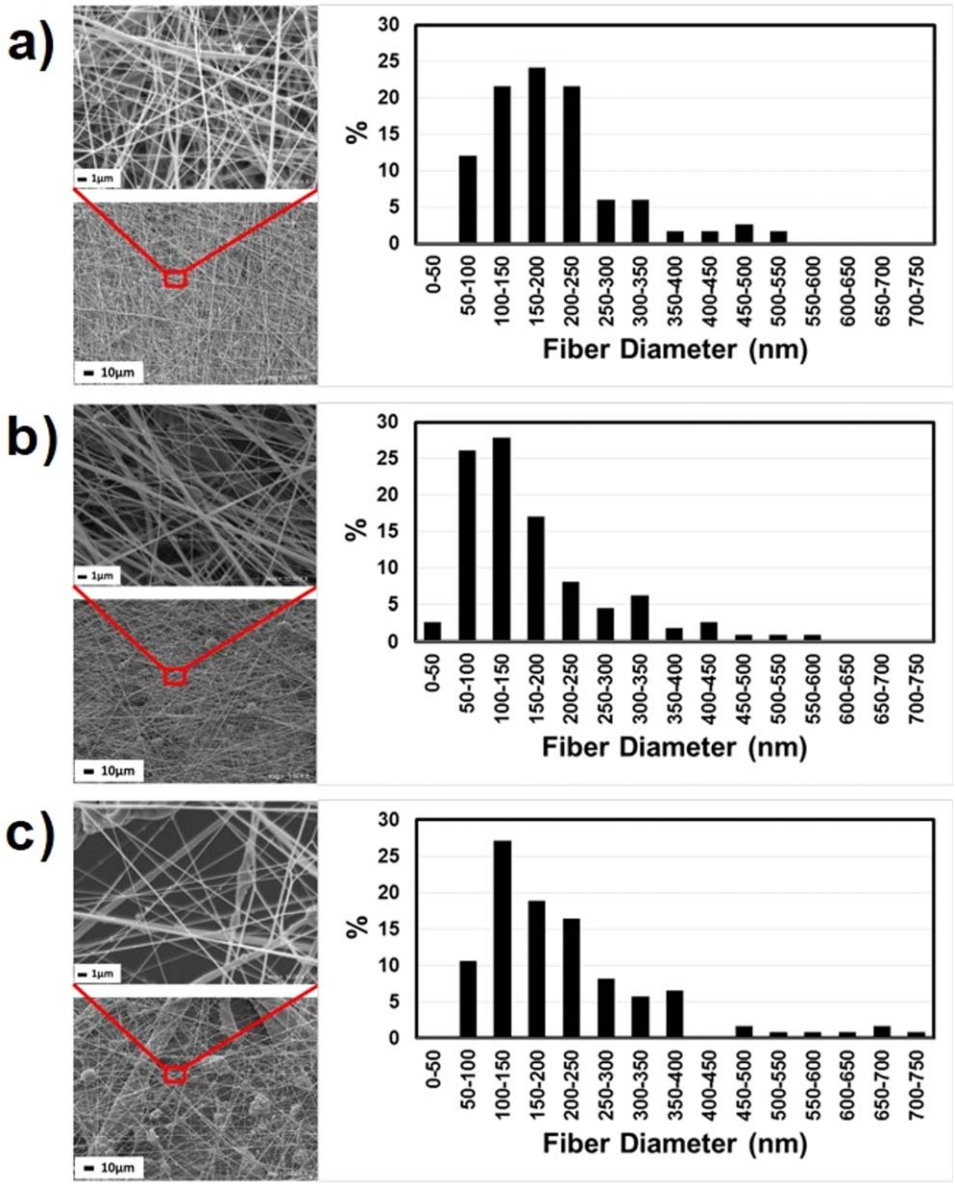

Figure 7. SEM images of solution-blown TPU fibers with working distances of (a) 15 cm (images of an area 5 cm from the central area are shown), (b) 30 cm, and (c) 50 cm. [Color figure can be viewed in the online issue, which is available at wileyonlinelibrary.com.]

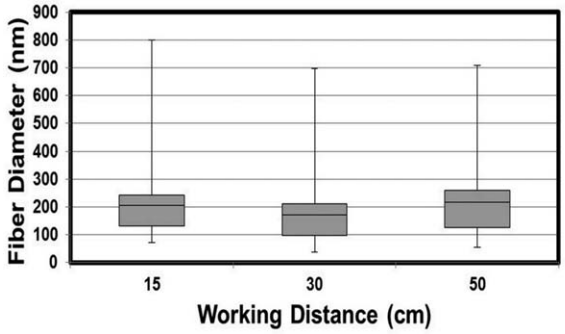

Parameters	Working Distance (cm)	Mean Diameter (nm)
P= 3bar	15	205±112
Q= 10mL/h	30	170±112
C= wt%10	50	218±131

Figure 8. Working distance between nozzle and collector vs. fiber diameter. The boundaries of the box plots indicate the 25th and 75th percentiles and the line indicates the median. The error bars above and below the box indicate the 95th and 5th percentiles. These data suggest that a working distance of 30 cm is optimal to achieve a smaller fiber diameter with a uniform distribution.

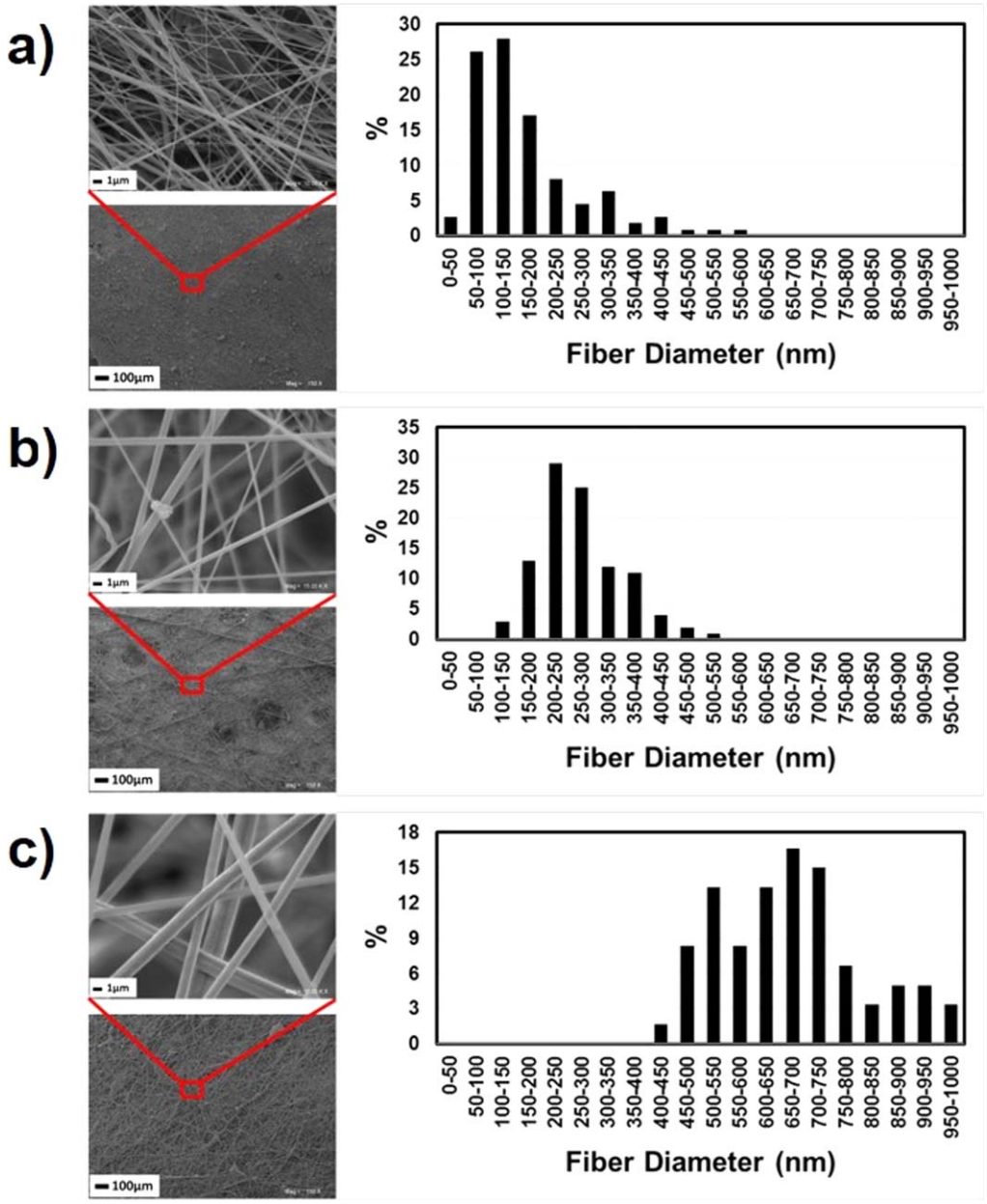

Figure 9. SEM images of solution-blown TPU fibers with different concentration values produced at (a) 10%, (b) 15%, and (c) 20%. [Color figure can be viewed in the online issue, which is available at wileyonlinelibrary.com.]

Effect of Flow-Rate

Following the optimization of the air pressure, the effect of varying the solution flow-rates, which are directly related to the productivity of the system, was investigated. The air pressure, nozzle-to-collector distance, and solution concentration were maintained at constant values while the solution flow-rate was varied between 1–50 mL/h, as indicated in Figure 4. The flow-rate did not significantly influence the nanofiber diameter; however, it affected the morphology of the TPU nanofiber (Figure 5). An increase in the flow-rate increased the level of bead formation because of the increased deposition through the nozzle.[6,10] The samples produced with flow-rates of 25 and 50 mL/h exhibited fiber agglomeration and high bead concentrations. This trend was more evident at a flow-rate of 50 mL/h, where an unexpected decrease in the fiber diameter was observed. This may be attributed to the agglomeration of the fibers, which was not considered when measuring the fiber diameter. The other two samples produced at flow-rates of 1 and 10 mL/h resulted in nanofiber webs with a more uniform fiber morphology. The samples produced at flow-rates of 1 and 10 mL/h exhibited similar morphologies; however, the productivity differed during their production. Thus, the optimal flow rate was determined to be 10 mL/h.

Effects of Working Distance

The distance between the nozzle and the collector determines the solvent evaporation time and thus the morphology and diameter of the fiber. The working distance was varied between

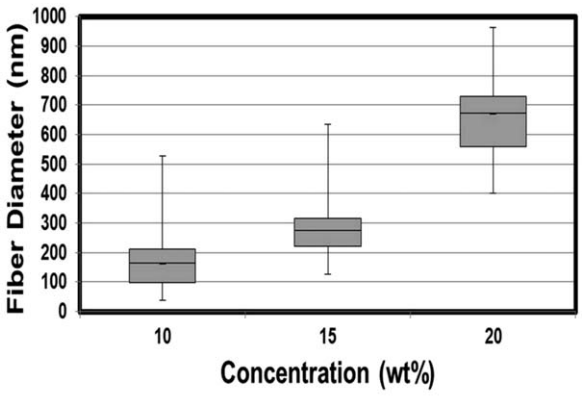

Process Parameters	Concentration (wt %)	Mean Diameter (nm)	Shear Viscosity [Mpa·s]
P = 3bar	10	170±112	347
d= 30cm	15	275±92	3245
Q= 10mL/h	20	671±136	13046

Figure 10. Effect of polymer solution concentration. The boundaries of the box indicate the 25th and the 75th percentiles and a line marks the median. The error bars above and below the box indicate the 95th and 5th percentiles. These data suggest that a polymer concentration of 10% is optimum for smaller fiber diameter.

15 and 50 cm while all the other parameters remained constant, as shown in Figure 7. The fiber web collected at a distance of 15 cm exhibited two areas with completely different morphologies. As shown in Figure 6(a), the central area of the sample where the jet strikes the collector was covered with droplets that formed a film-like structure on drying. It is likely that the film-like structure consisted of a mixture of fibers and droplets, where even the dried fibers dissolved into a film on reaching the collector. It is speculated that the formation of the nanofibers was restricted due to solvent evaporation and insufficient drawing of fibers. However, images captured at an area located 5 cm from the central area revealed that the air-flow system and comparatively longer distance resulted in the production of fibers with a similar morphology to those collected at a working distance of 30 cm [Figures 6(b) and 7(b)].

Over an identical period, fewer fibers were collected at a working distance of 50 cm compared with that of 30 cm. The greater working distance resulted in a loss of fibers, even when the maximum suction power was employed. Consequently, the optimal working distance was determined to be 30 cm for further experiments [Figure 8].

Effects of Solution Concentration

On the basis of the SEM analysis and observed fiber morphologies, the optimized process parameters could be summarized as an air pressure of 3 bar, polymer flow rate of 10 mL/h, and nozzle-to-collector distance of 30 cm. The amount of solvent in the TPU solution should be reduced to achieve greater productivity. Consequently, the solution concentration was increased to 15% and 20% for scalability analysis.

As expected, the polymer concentration greatly influences the nanofiber diameter (Figures 9 and 10). The finest fibers were obtained with the lower polymer concentrations. The fiber diameter drastically increased with polymer concentrations greater than 15 wt %. Under a concentration of 20 wt %, the average diameter of the obtained fibers was greater than 400 nm, which is in the micro-scale fiber range.

Table II. The Relationship between Fiber Diameter and Pearson Correlation for the Various Parameters

	Air Pressure	Flow-rate	Distance	Concentration
Diameter	−0.019	−0.139	0.001	0.565

The polymer concentration affects the process continuity and uniformity of the nanofibers, as well as the rheological behavior and morphology of the fibers because of the physical forces that are generated during the formation of the fibers. A low polymer concentration does not enable adequate chain entanglement, and beads are formed on the nanofiber surface unless the molecular weight is sufficient to maintain the viscosity of the solution [15]. As the molecular weight remained at a constant value, an increase in the polymer concentration led to an increase in the solution viscosity (Figure 10).

According to the Pearson correlation shown in Table II, the solution concentration has the greatest influence on the fiber diameter. The concentration strongly correlated with the fiber diameter ($r_p = 0.565$). In contrast, the other parameters showed a weak correlation with the r_p values, namely, the air pressure (−0.019), solution flow-rate (0.139), and distance (0.001).

Barrier Properties. The capillary-flow porometry method is used to investigate the porosity, which is one of the most critical properties of nanofiber webs. This method is more reliable compared with other methods such as SEM and AFM analysis, which primarily use image-processing techniques to investigate the pore size of nanofiber webs. These methods, which depend on image processing, can only analyze the upper (visible) layers of nanofiber webs. An evaluation of the upper layer merely provides superficial information on the pore size and pore size distribution of the nanofiber web. The polymer concentration, which is one of the major factors that affect productivity, was determined to have the greatest influence on the fiber diameter and web morphology. Consequently, the effect of the polymer concentration on the air permeability and porosity of the webs was investigated. This highlighted the possible use of solution-blown TPU nanofibrous webs for filtration purposes. As Table III shows, a correlation between the nanofiber diameters, mean pore size, air permeability, and polymer concentration can be considered. As

Table III. The Effect of Concentration on Air Permeability and Pore Size

Concentration (wt %)	Mean diameter (nm)	Air permeability @125Pa [$cm^3/cm^2.s$]	Pore size (μm)		
			max.	average	min.
10	170 ± 112	181.3 ± 23.4	10.5	4.7	2.2
15	275 ± 92	136.7 ± 59.2	35.3	4.2	2.4
20	671 ± 136	665.9 ± 22.7	40.9	8.5	3.4

expected, the nanofiber diameter increases as the polymer concentration is increased, which leads to an increase in the mean pore size. Consequently, the air permeability will increase as the mean pore size increases. However, the difference between the average fiber diameter of the 10 wt % and 15 wt % TPU samples was not sufficiently large. The air permeability and pore sizes of the aforementioned samples were almost identical; however, the blown web of the 20 wt % solution exhibited significantly higher values. This indicates that the mean pore size can be engineered by altering the polymer concentration, highlighting the great potential for the management of the barrier properties of nanofiber webs.

CONCLUSIONS

Nanofibrous TPU membranes were produced via SB. This study showed that SB is a practical and feasible method for the production of nanofibers. It can obtain fine nanofibers at high production rates without the use of high-voltage electrical charges. The morphologies and diameters of the fibers were analyzed by varying the process parameters, such as the air pressure, solution flow-rate, and working distance and by varying the concentration of the solution as a material parameter. The solution concentration had the most influence on the fiber diameter, whereas the air pressure had the greatest effect on the web uniformity and defect density. Polymer droplets were observed at lower air pressures; however, the air pressure did not linearly influence the diameter of the nanofibers. It is obvious from the obtained results that webs with modified pore sizes and air permeability can be simply controlled by changing the polymer concentration. For this particular set-up, the optimum air pressure value was determined to be 3 bar. An increase in the solution flow-rate resulted in the production of fibers with larger diameters and a greater amount of droplets. For an air pressure of 3 bar, the estimated optimum flow-rate was determined to be 10 mL/h, which can be increased by simply increasing the number of nozzles for industrial scalability. Enhanced productivity during nanofiber production will facilitate the use of such technical fabrics in applications such as filters, protective textiles, scaffolds, wound dressings, and battery components.

ACKNOWLEDGMENTS

The authors gratefully acknowledge the ITU Scientific Research Fund (ITU-BAP) for the financial support of this work. Thanks are also due to Prof. Oktay Yilmaz and Hasan Var for their analytical assistance and fruitful discussions.

REFERENCES

1. Teo, W. E.; Ramakrishna, S. *Nanotechnology* **2006**, *17*, R89.
2. Banuskeviciute, A. E.; Adomaviciute, R.; Milasius, Stanys, S. *Mater. Sci.* **2011**, *17*, 287.
3. Mary, L. A.; Senthilram, T.; Suganya, S.; Nagarajan, L.; Venugopal, J.; Ramakrishna, S.; Giri Dev, V. R. *Express Polym. Lett.* **2013**, *7*, 238.
4. Uppal, R.; Bhat, G.; Eash, C.; Akato, K. *Fibers Polym.* **2013**, *14*, 660.
5. Ellison, C. J.; Phatak, A.; Giles, D. W.; Macosko, C. W.; Bates, F. S. *Polymer* **2007**, *48*, 3306.
6. Zhang, L.; Kopperstad, P.; West, M.; Hedin, N.; Fong, H. *J. Appl. Polym. Sci.* **2009**, *114*, 3479.
7. Zhuang, X.; Shi, L.; Jia, K.; Cheng, B.; Kang, W. *J. Membr. Sci.* **2013**, *429*, 66.
8. Zhuang, X.; Yang, X.; Shi, L.; Cheng, B.; Guan, K.; Kang, W. *Carbohydr. Polym.* **2012**, *90*, 982.
9. Zhuang, X.; Jia, K.; Cheng, B.; Feng, X.; Shi, S.; Zhang, B. *Chem. Eng. J.* **2014**, *237*, 308.
10. Medeiros, E. S.; Glenn, G. M.; Klamczynski, A. P.; Orts, W. J.; Mattoso, L. H. *J. Appl. Polym. Sci.* **2009**, *113*, 2322.
11. Sánchez–Adsuar, M. S.; Papon, E.; Villenave, J.-J. *J. Appl. Polym. Sci.* **2000**, *76*, 1602.
12. Eceiza, A.; Martin, M. D.; De La Caba, K.; Kortaberria, G.; Gabilondo, N.; Corcuera, M. A.; Mondragon, I. *Polym. Eng. Sci.* **2008**, *48*, 297.
13. Gorji, M.; Jeddi, A.; Gharehaghaji, A. A. *J. Appl. Polym. Sci.* **2012**, *125*, 4135.
14. Li, D.; Frey, M. W.; Joo, Y. L. *J. Membr. Sci.* **2006**, *286*, 104.
15. Tan, S. H.; Inai, R.; Kotaki, M.; Ramakrishna, S. *Polymer* **2005**, *46*, 6128.